Clim Dyn (2018) 50:1413–1424
DOI 10.1007/s00382-017-3694-x

# Recent interdecadal shift in the relationship between Northeast China's winter precipitation and the North Atlantic and Indian Oceans

**Han Tingting**[1,2,4] · **He Shengping**[1,2] · **Hao Xin**[1,2,4] · **Wang Huijun**[1,2,3]

Received: 17 July 2016 / Accepted: 17 April 2017 / Published online: 25 April 2017


**Abstract** This study documents an interdecadal change in the interannual relationship between Northeast China's winter precipitation (NECWP) and the sea surface temperature (SST) in the North Atlantic and Indian Oceans in the 1990s. It is revealed that the NECWP shows a significant simultaneous correlation with the SST anomalies in the North Atlantic (SST_Atlantic)/tropical Indian Ocean (SST_Indian) during 1996–2013/1961–1990. Generally, the NECWP anomaly is concurrent with apparent Eurasian wave pattern during 1961–1990 whereas anomalous Okhotsk high and East Asia trough during 1996–2013. It is found that, before the 1990s, the warming SST anomalies in the tropical Indian Ocean could stimulate the Eurasian wave pattern via inducing significant anomalous upper-level convergence over the northern Europe, which tends to favor a positive NECWP anomaly. During 1996–2013, the SST_Indian-NECWP connection is disrupted. Instead, the North Atlantic tri-polar SST anomaly pattern exerts a dominant impact on the NECWP through triggering a stationary Rossby wave that originates from the North Atlantic and propagates eastward to Northeast Asia and further modulates the Okhotsk high and East Asia trough. Further analyses indicate that the weakened connection between the tropical SST_Indian anomalies and the northern Ferrell circulation likely contributes to the weakening of the NECWP–SST_Indian relationship after the 1990s. However, the eastward shift and the enlarged anomalous magnitudes of the North Atlantic Oscillation might favor the strengthening of the NECWP–SST_Atlantic relationship after the mid-1990s. It is therefore suggested that the strengthened variability of the SST_Atlantic anomalies after the 1990s might partially contribute to the intensification of the interannual variability of the NECWP.

**Keywords** SST · Northeast China's winter precipitation · Interdecadal shift · Interannual variability

## 1 Introduction

Northeast China (NEC) is one of China's grain production bases. Climate variability in this region, especially precipitation variability, is of great importance for crops yields, industrial production, social ecosystems and economics. Precipitation in NEC exhibits not only the entanglement of spatial heterogeneity and regional diversity but also the coexistence of interannual and interdecadal variabilities (Sun et al. 2000; Gong et al. 2006).

Located in the mid- to- high-latitudes, precipitation in NEC is affected by the atmospheric circulation anomalies in both the tropical and extratropical regions such as blockings in the high-latitudes (Yao and Dong 2000), the cold vortex (Shen et al. 2011), the East Asian monsoon circulation (Guo 1983; Sun et al. 2002), the soil moisture content in northwest Eurasia (Zhu 2011), and the North

✉ Han Tingting
hantt08@126.com

[1] Nansen-Zhu International Research Centre, Institute of Atmospheric Physics, Chinese Academy of Sciences, 100029 Beijing, China

[2] Climate Change Research Center, Chinese Academy of Sciences, 100029 Beijing, China

[3] Collaborative Innovation Center on Forecast and Evaluation of Meteorological Disasters/Key Laboratory of Meteorological Disaster, Ministry of Education, Nanjing University for Information Science and Technology, 210044 Nanjing, China

[4] University of Chinese Academy of Sciences, 100049 Beijing, China

Atlantic Oscillation (NAO; Sun and Wang 2012). Shen and Lian (2004) indicated that the precipitation in NEC may be related to the snow cover on the Tibetan Plateau. The behaviors of the cold vortex in NEC generally contribute to precipitation variability, and the cold vortex is related to the North Pacific Oscillation (Liu et al. 2002) and the Northern Hemisphere annual mode (He et al. 2006). Additionally, Gao et al. (2014) suggested that the precipitation anomalies in the Huang-Huai region in late spring could cause the local soil moisture anomalies and then generate summer general circulation anomalies, which lead to anomalous summer precipitation in NEC. Wang and He (2013) associated the increase in snowfall in NEC around the mid-1980s with the weakening of the East Asian winter monsoon. Recently, Han et al. (2015) revealed that there was a decrease of summer precipitation in NEC after the late-1990s, and they attributed this to the weakened northeast summer monsoon circulation and the changes in the Arctic sea ice cover. This decadal decrease is also related to the phase shift of the Pacific decadal oscillation (Xu et al. 2015). Wang and He (2015) analyzed the North China/Northeast Asia severe drought in the summer of 2014 and indicated that it was the joint result of Pacific sea surface temperature (SST) anomalies, Arctic sea ice anomalies and warming over the European continent and the Caspian Sea.

There are also a number of publications concerned with the relationships between climate variability in NEC and SST (Geng et al. 1997; Liu and Wang 2001; Hu et al. 2003; Feng et al. 2006; Sun and Wang 2006). For example, Bai (2001) found that the meridional difference between the north and south SST in the North Atlantic affects the precipitation in NEC via the anomalous blocking and westerlies circulation in East Asia. Cao et al. (2013) determined that the SST contrast between the tropical Indian Ocean and the tropical western Pacific exerts a robust and strong influence on the precipitation in Northeast China through the significant meridional teleconnection pattern of lower-tropospheric circulation anomalies over the western North Pacific and East Asia. This is consistent with the work by Li et al. (2013), who documented that the influences of the Indian Ocean SST and Pacific SST on summer precipitation in China are qualitatively opposite. Zhou and Wang (2014) stated that the warming SST anomaly in the Kuroshio region results in a weakened polar vortex and a strengthened western Pacific subtropical high and consequently results in more precipitation in NEC. However, such relationships may not be stable. Wu et al. (2010, 2011) reported that the influence of a developing ENSO on NEC temperature was prominent before the late-1970s, whereas the impact of the North Atlantic SST became more important in the 1980s and 1990s. Furthermore, the correlation between the ENSO and seasonal mean precipitation in NEC is unstable (Wu et al. 2003). Based on atmospheric general circulation model experiments, Chang et al. (2013) proposed that the linear relationships between Northeast Asian summer precipitation and tropical basin SST diminish when the location of the ocean basin is shifted from west to east. Therefore, it is of particular significance to explore the decadal change of the associated regional SST with precipitation in NEC on the interannual time scale, which is the purpose of this work. More attention has been directed at the relationships between summer precipitation and the SST; therefore, it is essential to focus on the correlated SST with winter precipitation in NEC.

This study is structured as follows. Section 2 introduces the datasets and methods in this study. Section 3 illustrates the interdecadal change of the associated regional SST with winter precipitation in NEC. Brief conclusions are provided in Sect. 4.

## 2 Data and methods

The monthly atmospheric reanalysis dataset used in this study comes from the National Center for Environmental Prediction/National Center for Atmospheric Research (NCEP/NCAR) global atmospheric reanalysis data for 1948–2014 at a resolution of 2.5°×2.5° (Kalnay et al. 1996). The monthly SST dataset on a 2.0°×2.0° latitude/longitude grid is the National Oceanic and Atmosphere Administration (NOAA) Extended Reconstructed SST V4b for 1854–2014 (Huang et al. 2015). An advanced monthly precipitation observation dataset over China, CN05.1 (Wu and Gao 2013), is also used in the study. The dataset is constructed based on an interpolation from more than 2400 observation stations in China and has a relatively high resolution of 0.5°×0.5° for 1961–2014. Another precipitation data set is NOAA's Precipitation Reconstruction over Land (PREC/L) at a resolution of 1.0°×1.0° for 1961–2014 (Chen et al. 2002). Given that recently, the interannual variability of NEC precipitation has strengthened in December and January (figure not shown), we focused on early winter (December and January) in this study. For example, the winter of 1961 refers to the average of December 1961 and January 1962. The common time period in this study is 1961–2013.

Here, NEC is defined as the region north of 38°N and east of 115°E in China. The winter precipitation in the NEC (NECWP) index is defined as the normalized interannual component of the area-averaged precipitation in NEC during early winter, based on the CN05.1 dataset. To emphasize the interannual variability, all of the data were filtered using the Butterworth 11 year high-pass filter before being analyzed. The two-tailed $F$ test was applied to statistically test the significance of the difference in interannual

variability, and Student's *t* test was used to detect the significance in the regression and correlation analyses.

## 3 Interdecadal shift in the relationship of the NECWP with the North Atlantic and Indian Oceans

As shown in Fig. 1a, the simultaneous SST associated with the NECWP displays a tri-polar pattern in the North Atlantic for 1961–2013, although the positive correlations in the mid-latitude Atlantic are weak. We defined the SST_Atlantic index as follows:

$$\mathrm{SST\_Atlantic} = \left[\mathrm{SST}_{(40^\circ\sim50^\circ\mathrm{N},30^\circ\sim60^\circ\mathrm{W})} + \mathrm{SST}_{(5^\circ\sim15^\circ\mathrm{N},15^\circ\sim50^\circ\mathrm{W})}\right] \times 0.25 - \mathrm{SST}_{(20^\circ\sim36^\circ\mathrm{N},15^\circ\sim90^\circ\mathrm{E})} \times 0.5.$$

Figure 1b displays the time series of the NECWP (the blue solid line) and SST_Atlantic (the red dashed line) indices. It is notable that the relationship between the two indices varies with time and that the in-phase co-variability occurs after the 1990s. We also calculated the 17-year-sliding correlation coefficients between the two indices. It suggests that the NECWP–SST_Atlantic correlations are negative but insignificant before the 1990s and then become positive after the 1990s. The positive correlations strengthen sharply and become statistically significant after the mid-1990s. Based on the changes in the NECWP–SST_Atlantic relationship after the 1990s and in order to avoid the effect of choosing the sliding window width, we present two periods, 1961–1990 [P1] and 1996–2013 [P2], by removing the middle transitional five years, to demonstrate the decadal change of the NECWP–SST_Atlantic relationship. As shown in Fig. 2, during P1, negative correlations occupy the partial mid-latitude Atlantic with slight positive correlations in the subtropical Atlantic. This implies the weak negative correlations of the NECWP index with the SST_Atlantic index before the 1990s (Fig. 1c). After the mid-1990s, significant positive correlations are located in

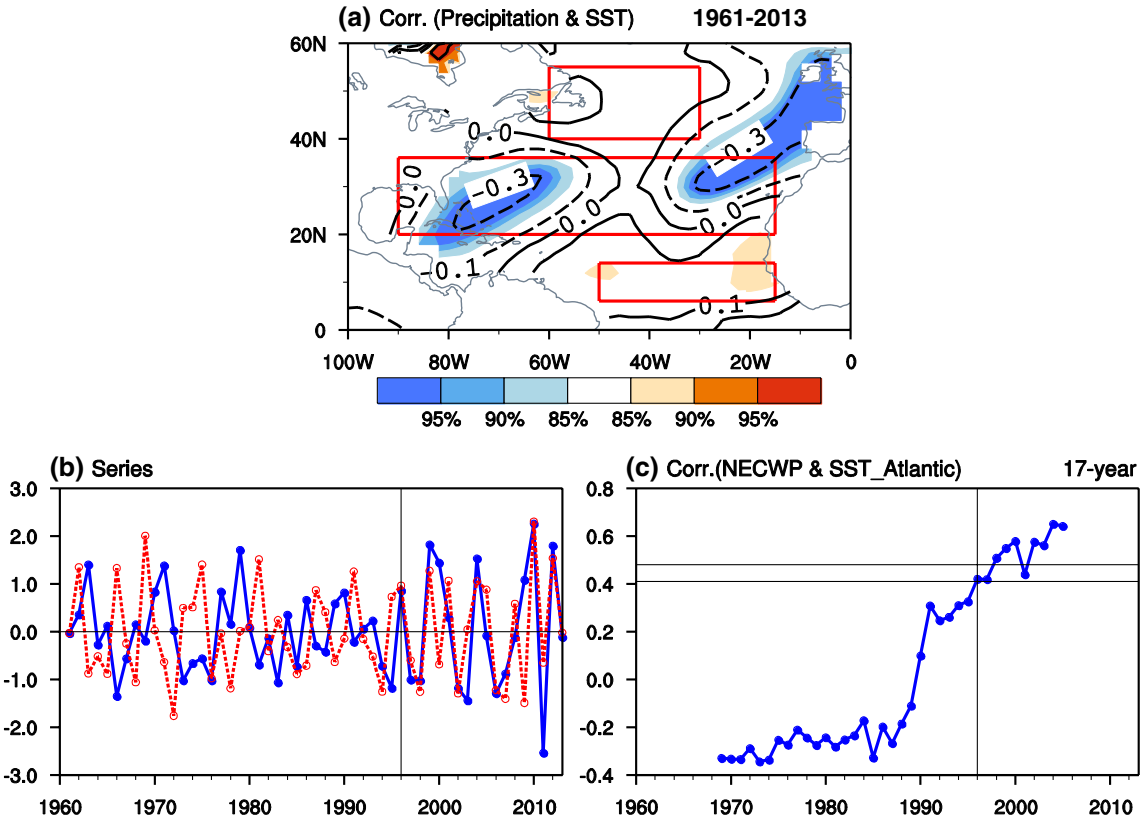


**Fig. 1** **a** Geographical distribution of the correlation coefficients between the winter sea surface temperature (SST) and the winter precipitation in the Northeast China (NECWP) index for 1961–2013. *Shadings* indicate values significantly exceeding the 95, 90 and 85% confidence levels through Student's *t* test, respectively. The rectangular areas are the selected key regions. **b** The time series of the normalized NECWP (*blue solid line*) and SST_Atlantic (*red dashed line*) indices during 1961–2013. **c** The 17-year-sliding correlation coefficients between the NECWP and SST_Atlantic indices. The *solid horizontal lines* denote the 95 and 90% confidence levels, as estimated using Student's *t* test

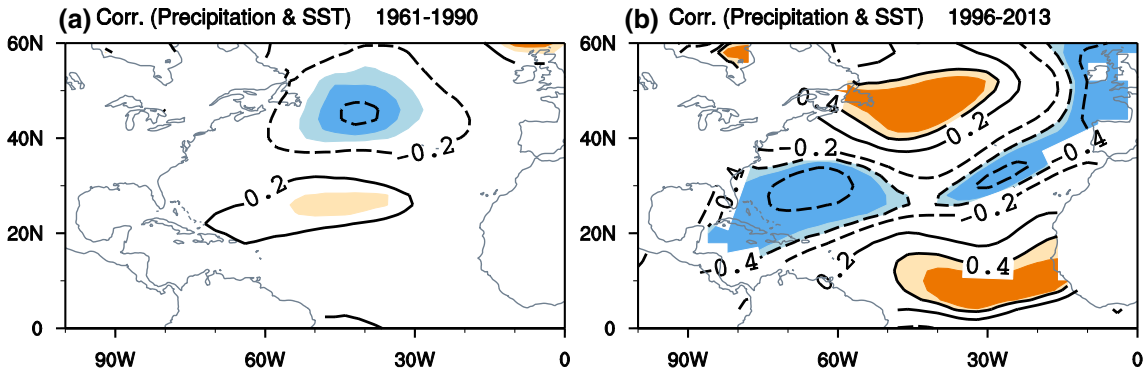


**Fig. 2** Geographical distribution of the correlation coefficients between the winter SST in the North Atlantic and the NECWP index during **a** 1961–1990 and **b** 1996–2013. *Dark* (*light*) *shadings* indicate values significantly exceeding the 95% (90%) confidence level, estimated by Student's *t* test

the mid-latitude and tropical Atlantic, with negative correlations in the subtropical Atlantic. The NECWP-related SST anomalies behave in a tri-polar pattern in the Atlantic, which manifests significant co-variability between the two indices after the mid-1990s (Fig. 1c). The results show that the tri-polar SST anomaly pattern in the Atlantic dose not have an intimate connection with winter precipitation over NEC until the 1990s. Hence, we speculated that SST in other regions may be related to the NECWP before the 1990s. As illustrated in Fig. 3a, the tropical Indian Ocean SST is closely associated with the NECWP for 1961–1990. To facilitate the analysis, the SST_Indian index was defined by averaging the SST of significance in the tropical Indian Ocean. As shown in Fig. 3b, the SST_Indian index covaries with the NECWP index before the 1990s ($R=0.51$; above 99% confidence interval), whereas the in-phase covariability disappears afterward ($R=-0.14$ for 1996–2013; not significant), which is also verified by their 17-year-sliding correlation coefficients (Fig. 3c). These results indicate that the regional SST associated with winter precipitation in NEC changes in the 1990s. It is the tropical Indian Ocean SST anomalies that are of importance for winter precipitation in NEC before the 1990s, whereas after that, the tri-polar SST anomalies in the North Atlantic become vital.

To further illustrate the different impacts of the North Atlantic/Indian Ocean on the NECWP between the two sub-periods, we examined the associated atmospheric circulation anomalies with the SST_Indian and SST_Atlantic indices in this section. Figure 4 illustrates the features of the linear regression of simultaneous geopotential height at 500 hPa (Z500) and horizontal winds at 850 hPa (UV850) against the NECWP and the SST_Indian indices. During P1, when warming SST anomaly occurs in the tropical Indian Ocean, in the middle troposphere, positive geopotential height anomalies dominate Europe, northern and northeastern China, and Northwest Pacific, along with negative values over Siberia, exhibiting a Eurasian wave train pattern (EU pattern) over the mid- to high-latitudes (Fig. 4b). Meanwhile, the positive precipitation anomaly is associated with the similar wave train pattern of anomalous geopotential height in the middle troposphere (Fig. 4a). Correspondingly, the appearance of "anticyclone"–"cyclone"–"anticyc lone" can be observed over the mid- to high-latitudes in the low-level horizontal wind anomalies associated with the SST_Indian and NECWP indices (Fig. 4c, d). Anomalous southerlies extend along eastern China and transport water vapor originating from the tropics northward into NEC. Additionally, the Indian Ocean is an important water vapor source for precipitation processes in eastern China (Wang and Chen 2012; Sun and Wang 2015). Hence, the associated moisture conditions were explored. In 1961–1990, water vapors associated with winter precipitation in NEC are from the inland across the western boundary and from the tropical Indian Ocean and West Pacific across the southern boundary. The positive SST_Indian index is also characterized by an anomalous westerly current across the western boundary and a southwesterly current across the southern boundary over NEC. The anomalous westerly that flows over the northern Indian Ocean transports the warm and wet current northeastward and then invades NEC, which increases the water vapor content and consequently the precipitation.

The thermal condition of the Indian Ocean is an important factor that can affect the Asian climate. Based on observations and the ECHAM5 atmospheric general circulation model, Xu and Fan (2012, 2014) showed that the Indian Ocean SST interannual variability mode can influence the precipitation over the middle reach of the Yangtze River and South China via anomalous circulation and water vapor transport. The question is how the Indian Ocean SST induces the extratropical wave pattern of atmospheric circulation anomalies to affect the early-winter precipitation over NEC in Fig. 4b. To explore the potential effect of the

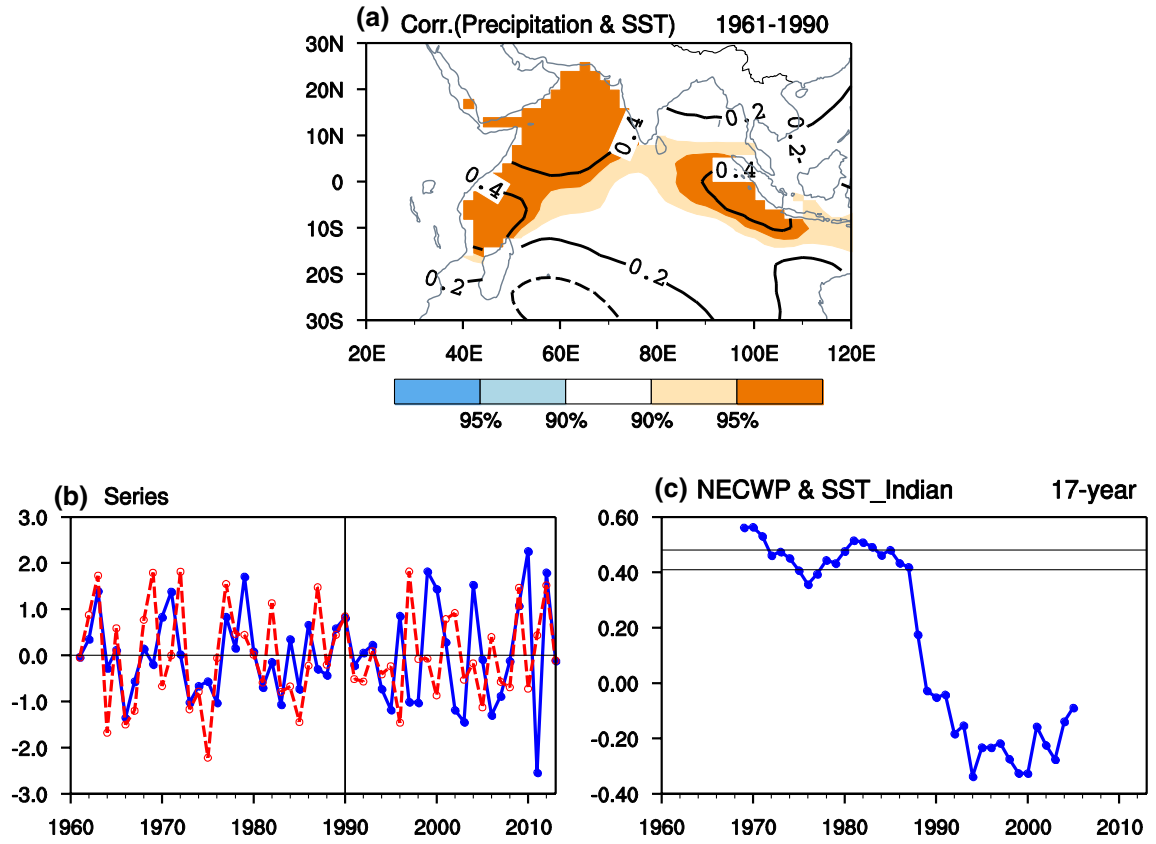


**Fig. 3** **a** Geographical distribution of correlation coefficients between the winter SST in the tropical Indian Ocean and the NECWP index during 1961–1990. *Dark* (*light*) *shadings* indicate values significantly exceeding the 95% (90%) confidence level, estimated by Student's *t* test. **b** The time series of the normalized NECWP (*blue solid line*) and SST_Indian (*red dashed line*) indices during 1961–2013. **c** The 17-year-sliding correlation coefficients between the NECWP and SST_Indian indices. The *solid horizontal lines* denote the 95 and 90% confidence levels, estimated by Student's *t* test

Indian Ocean on the formation of the EU pattern, we investigated the anomalous upper-level divergence and Rossby wave source (RWS) associated with the SST_Indian index. Figure 5 shows the SST_Indian-related patterns of diverse variables during 1961–1990. The notable feature is the prominent upper-level convergence and RWS anomalies over the northern Europe and the eastern Mediterranean Sea in response to a positive SST_Indian index, which is consistent with the divergence anomalies at the near-surface level. In addition, the near-surface divergence (convergence) anomalies are consistent with the high (low) SLP anomalies that are associated with SST anomalies in the tropical Indian Ocean. Sardeshmukh and Hoskins (1988) have proposed that the advection of vorticity by the divergence anomalies can excite the Rossby wave. As shown in Figs. 4 and 5, the upper-level RWS anomalies are well consistent with where the anomalous divergence is located, accompanied by a set of wave trains over the downstream regions. Thus, the EU wave pattern associated with the tropical Indian Ocean SST anomaly is driven.

The following question is raised: why does the SST_Indian show a significant connection with atmospheric circulation at the mid- to- high-latitudes before the 1990s? Figure 6 displays the linear regression of the early-winter zonal mean mass stream function with regard to the SST_Indian index. In 1961–1990, the positive SST_Indian index is consistent with the significant northern Hadley and Ferrell cells, which suggests a strong coupling between the tropics and the mid- to- high-latitudes of the Northern Hemisphere. The SST_Indian might modulate the atmospheric circulation over the Eurasian continent and the NECWP through its impact on the northern meridional circulations. By contrast, in 1996–2013, the connection between the Indian Ocean SST and the northern Ferrell circulation has been weakened. Hence, the SST_Indian signal is faint over the Eurasian mid- to- high-latitudes (figure not shown). On the other hand, given that the tropical Pacific and Atlantic oceans might also contribute to meridional circulation anomalies that are concurrent with the Indian Ocean SST anomaly, we further examined the

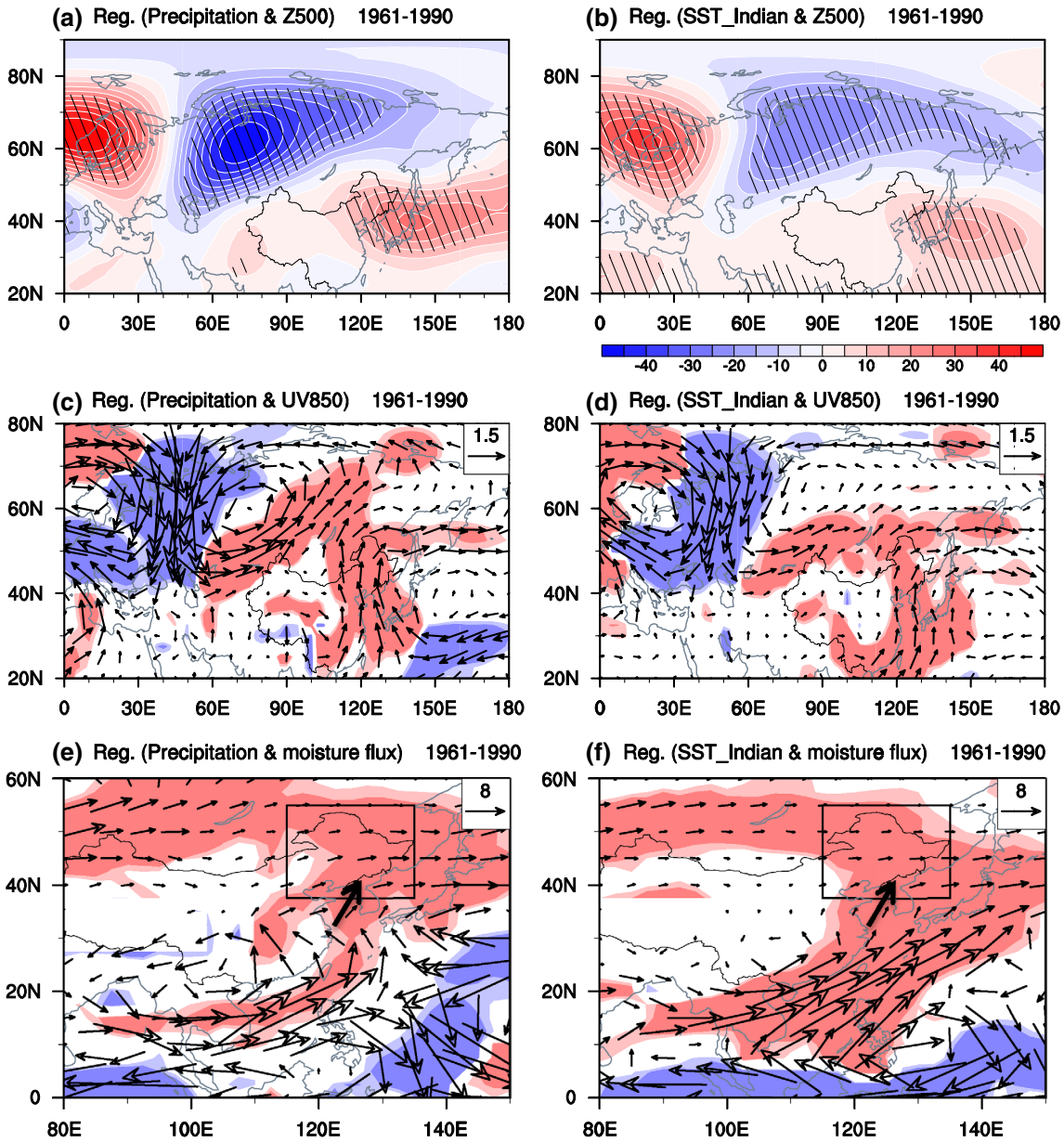


**Fig. 4** The linear regression pattern of the winter geopotential height at 500 hPa (Z500: m) against **a** the NECWP index and **b** the SST_Indian index for 1961–1990. The hatch areas indicate values significantly exceeding the 90% confidence level using Student's *t* test. The linear regression pattern of the winter horizontal wind at 850 hPa (UV850: m $s^{-1}$) against **c** the NECWP index and **d** the SST_Indian index for 1961–1990. **e**, **f** Same as **c**, **d** except for the vertically integrated moisture flux (kg $m^{-1}$ $s^{-1}$). *Dark* (*light*) *shadings* indicate values significantly exceeding the 95% (90%) confidence level, estimated by Student's *t* test

residual meridional circulation related to the Indian Ocean SST anomaly after removing the tropical Pacific and Atlantic signals. ENSO has been considered as the most striking interannual climate variation over the Pacific. When the ENSO signal is removed, the connection between the Indian Ocean SST and Hadley circulation has been weakened dramatically during both sub-periods (Fig. 7a). Interestingly, the Indian Ocean SST anomaly still shows a significant correlation with the northern Ferrell circulation during P1 (Fig. 7a), which is rarely observed during P2 (Fig. 7b). It is therefore speculated that the distinctive relationship between the Indian Ocean SST anomaly and the Ferrell circulation in the two sub-periods is not attributed to the tropical Pacific effect. Similarly, the influence of the Indian Ocean SST anomaly on the Ferrell circulation during the two sub-periods shows few changes when the tropical Atlantic effect has been removed (figures not shown). These results suggest that the tropical Indian Ocean has an

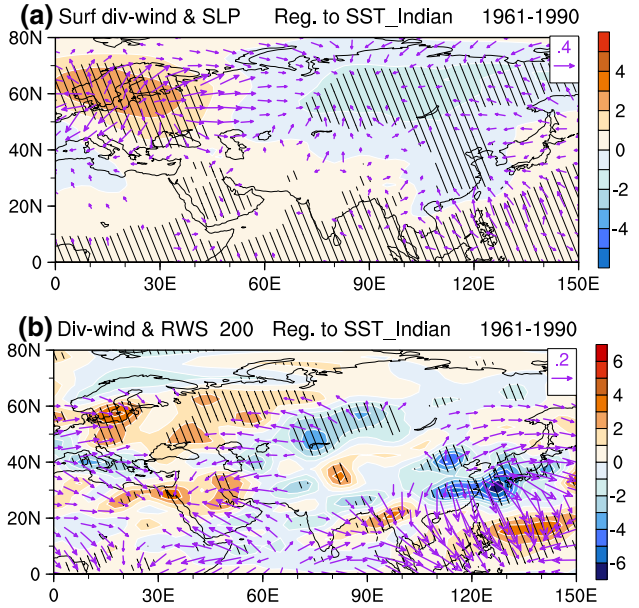


**Fig. 5** Regressions of **a** sea level pressure (SLP *shadings*: hPa) and **b** 200 hPa Rossby wave source (RWS *shadings*: $10^{-11}$ $s^{-2}$) anomalies onto the SST_Indian index for the early winter during 1961–1990. Vectors indicate **a** near-surface and **b** 200 hPa divergent wind component (m $s^{-1}$). Vectors with magnitudes less than 0.1 are not plotted

important influence on the decadal change of the meridional circulation anomalies. Hence, the weakened connection between the tropical Indian Ocean and the northern Ferrell circulation likely contributes to the weakening of the NECWP–SST_Indian relationship.

After the mid-1990s, the connection between the tropical Indian Ocean and the NECWP weakens, and the tri-polar SST anomalies in the North Atlantic show a close correlation with the NECWP. Figure 8 illustrates the features of the linear regression of Z500 and UV850 against the NECWP and the SST_Atlantic indices. The positive SST_Atlantic index is characterized by primarily positive geopotential height anomalies over the Okhotsk Sea and significant negative fluctuations over eastern China. Anomalous anticyclones occur over Siberia and the Okhotsk Sea. The easterly flows in the south flank of the anticyclone transport warm moist current from the Northwest Pacific into NEC. After the mid-1990s, the NECWP-related regimes change to the Okhotsk high and the East Asia trough. The anomalous easterlies carry warm wet air across the eastern boundary into NEC, which is the major water vapor source for the NECWP (figure not shown). Therefore, the SST_Atlantic-associated circulation anomalies are in accordance with the regimes that influence the winter precipitation in NEC.

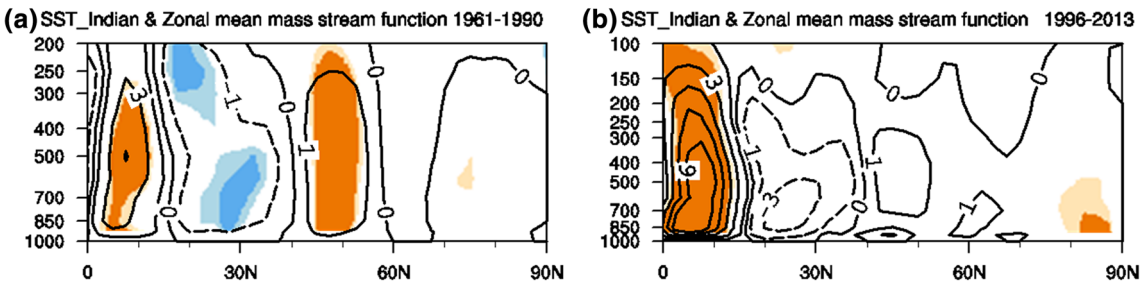


**Fig. 6** The linear regression pattern of the winter zonal mean mass stream function ($10^9$ kg $s^{-1}$) with regard to the SST_Indian index for **a** 1961–1990 and **b** 1996–2013. *Dark* (*light*) *shadings* indicate values significantly exceeding the 95% (90%) confidence level, estimated by Student's *t* test

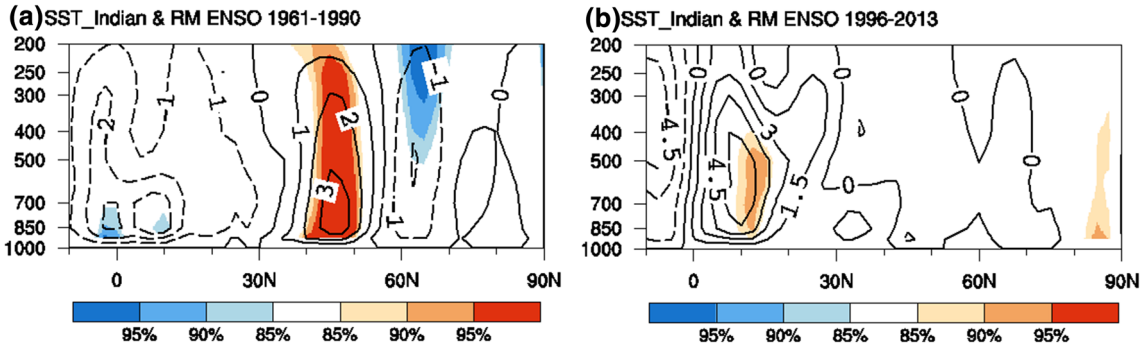


**Fig. 7** The linear regression pattern of the winter zonal mean mass stream function ($10^9$ kg $s^{-1}$) with regard to the SST_Indian index after removing ENSO signal for **a** 1961–1990 and **b** 1996–2013

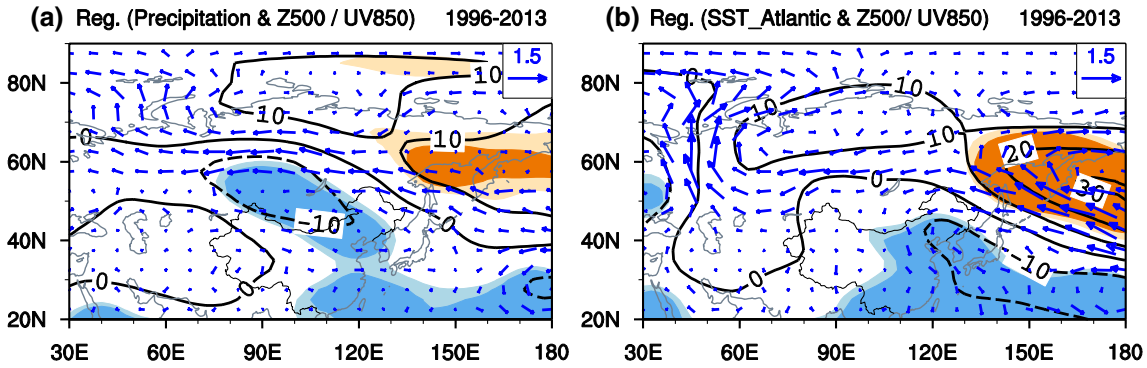


**Fig. 8** The linear regression pattern of Z500 (*contours*: m) and UV850 (*vectors*: m $s^{-1}$) against **a** the NECWP index and **b** the SST_Atlantic index for 1996–2013. *Dark* (*light*) *shadings* indicate values significantly exceeding the 95% (90%) confidence level, estimated by Student's *t* test

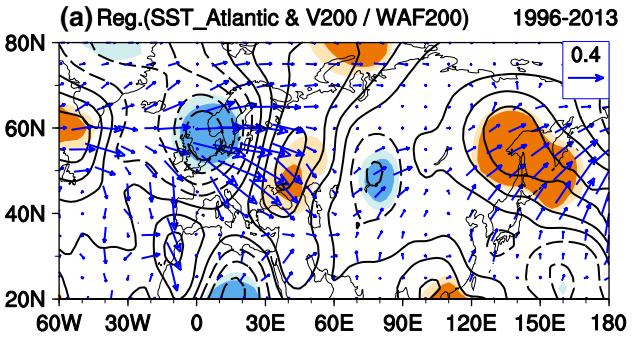


**Fig. 9** Regression maps of the winter meridional wind (*contours*: m $s^{-1}$) and wave activity flux (*vectors*: $m^2$ $s^{-2}$) at 200 hPa with regard to the SST_Atlantic index for 1996–2013. *Dark* (*light*) *shadings* indicate values significantly exceeding the 95% (90%) confidence level, estimated by Student's *t* test

Previous studies suggest that the Atlantic SST anomalies exert great impacts on the atmospheric circulation over East Asia via the Rossby wave pattern (Sun et al. 2008; Tian and Fan 2013; Zhou et al. 2013). The upper-layer meridional wind can depict zonally oriented teleconnections quite well (Watanabe 2004). Figure 9 shows the regression of 200 hPa meridional wind (V200: contours) and wave activity flux (WAF: vectors) computed according to Plumb's formulation (Plumb 1985) with regard to the SST_Atlantic index. The WAF can describe the propagation of stationary Rossby waves. One of the conspicuous features in Fig. 9 is that alternating anomalous northerly and southerly winds emanate eastward to East Asia and the Okhotsk Sea. Correspondingly, a wave pattern starts from the Atlantic and propagates eastward to Europe. This wave pattern bifurcates into two branches with one turning southeastward and equatorward to North Africa and the other extending eastward over the Eurasian continent. The latter can diffuse into Northeast Asia through an arch path. The Rossby wave pattern between the Atlantic and Northeast Asia, which is driven by the tri-polar SST anomaly pattern in the North Atlantic, can be evidence for such a remote relationship between the Atlantic signal and the climate in NEC.

The influence of the NAO on climate over Eurasia has been documented by previous studies (Hurrell 1995). It is speculated that the interdecadal change in the NCEWP–SST_Atlantic relationship might be related to the air-sea interaction in situ. Figure 10 depicts the SST_Atlantic-related sea level pressure (SLP) anomalies in the North Atlantic regions for the two sub-periods. For both sub-periods, SLP anomalies obtained from the regression and composite results exhibit a meridional dipole pattern with two active centers mainly over the North Atlantic, which resembles the NAO pattern. It is consistent with the previous study by Peng et al. (2003), who suggested that the North Atlantic tri-pole SST anomalies induce an NAO pattern via a dipolar anomalous eddy forcing. However, the NAO pattern changes substantially during 1996–2013 compared with that in 1961–1990. The most prominent distinction is that the extent of the two active centers enlarges eastward and anomalous magnitudes are remarkably enhanced, especially in the northern active center. Li et al. (2006) revealed that the positive feedback between the atmospheric anomaly and the North Atlantic tri-polar SST pattern can intensify the NAO response. The intensification of the NAO pattern associated with the SST_Atlantic implies that the air-sea interaction becomes stronger over the North Atlantic regions during 1996–2013. These changes might contribute to the strengthened NECWP–SST_Atlantic relationship.

The interdecadal shift of the interannual relationship between the NEC precipitation and the North Atlantic/Indian Oceans can also be recognized by the Fig. 11. During P1, when warming SST anomaly occurs in the tropical Indian Ocean, significant positive precipitation anomalies occupy NEC; whereas during P2, the precipitation anomalies become insignificant and negative over NEC excluding the small southwestern partion. Meanwhile, during P1, the

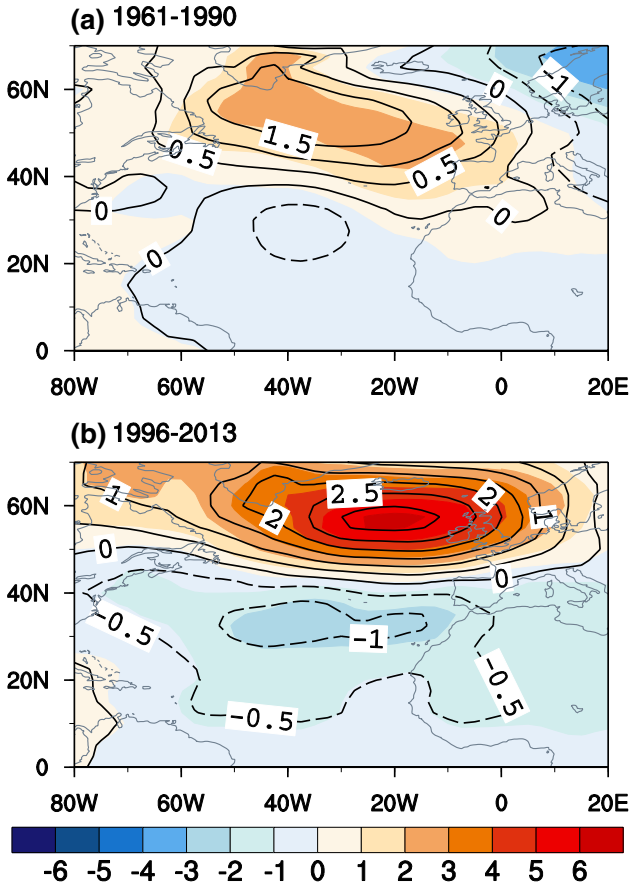


**Fig. 10** Composite differences (*shadings*: mb) of the winter sea level pressure (SLP) between the positive and negative SST_Atlantic index and the linear regression pattern (*contours*: mb) of SLP against the SST_Atlantic index in the period of **a** 1961–1990 and **b** 1996–2013

positive SST_Atlantic index correspondes to weak negative precipitation anomalies in most NEC. Significant anomalies only prevail over the small region of the central and southwestern NEC. By contrast, during P2, the positive SST_Atlantic index is accomponied by strongly positive precipitation anomalies in NEC, especially the northern partion.

These above results show that the SST that is closely associated with the NECWP changes from the SST anomaly in the tropical Indian Ocean to the tri-polar SST anomaly pattern in the North Atlantic around the mid-1990s, which induces the decadal changes of the atmospheric circulations related to the NECWP. Specifically, it is the EU wave pattern over the Eurasian mid- to- high-latitudes that influences the NECWP in 1961–1990. By contrast, in 1996–2013, the effect of the Okhotsk high and East Asia trough on the NECWP are dominant, which is induced by the North Atlantic tri-polar SST anomaly. Additionally, Fig. 12 depicts the 11-year-sliding standard deviation of the SST_Atlantic index. It shows that the interannual variability of the SST_Atlantic has strengthened after the 1990s. As the SST_Atlantic exerts a great impact on the NECWP after the 1990s, the strengthened interannual variability of the SST_Atlantic may contribute to increased variability of the NECWP to some extent. Figure 13a, b show the differences (P2 minus P1) of the interannual variability of the winter precipitation in NEC based on the CN05.1 gridded data and the PREC/L data, respectively. The interannual variability is defined as the standard deviation of the winter precipitation. Consistent changes are observed between these two data sets: a significant increasing in the interannual variability has occurred after the 1990s. We also examined the 11-year-sliding standard deviation of the NECWP index (Fig. 13c). The result confirms that the interannual variability of the NECWP has strengthened after the 1990s. The standard deviation of the NECWP index increases from 0.78 for 1961–1990 to 1.38 for 1996–2013 with a statistical $F$ test of 3.24, which is above 0.01 confidence level ($F = 2.95$).

## 4 Conclusions

This study investigates the interdecadal shift in the interannual relationship of the NECWP with the SST in the North Atlantic and the tropical Indian Ocean around the 1990s. It is the winter SST anomalies in the tropical Indian Ocean that are important to the NECWP during 1961–1990, whereas the tri-polar SST anomaly pattern in the North Atlantic becomes vital in 1996–2013. Specifically, during 1961–1990, the warming SST anomalies in the tropical Indian Ocean can cause significant anomalous divergence over the northern Europe. As the advection of vorticity by the divergence anomalies can excite the Rossby wave (Sardeshmukh and Hoskins 1988), the EU wave pattern of atmospheric anomalies is observed over the Eurasian mid- to- high-latitudes. Through this pathway, warming SST anomalies in the tropical Indian Ocean are together with intensified transportation of moisture across the western and southern boundaries, which tend to favor positive NECWP anomalies. During 1996–2013, the connection between the tropical Indian Ocean and the NECWP weakens, whereas the North Atlantic shows a close association with the circulations over Northeast Asia and the NECWP. The North Atlantic tri-polar SST anomalies can trigger a stationary Rossby wave originating from the North Atlantic and propagating eastward to Northeast Asia through an arch path. The positive SST_Atlantic index is associated with the enhanced Okhotsk high and the deepened East Asia trough along with the anomalous easterly current from the Northwest Pacific, which are dominant for the positive precipitation anomaly.

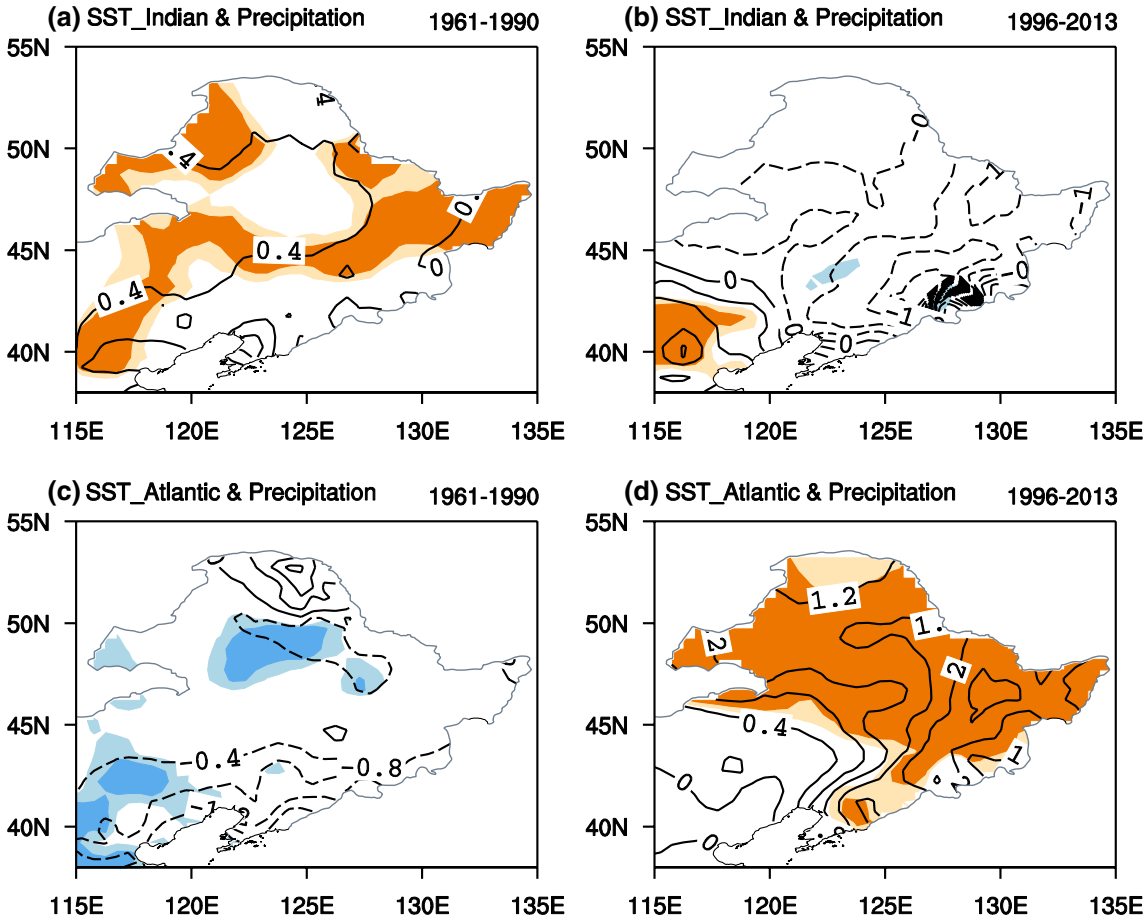


**Fig. 11** Regression maps of the early-winter precipitation in NEC with reference to the SST_Indian and the SST_Atlantic indices during **a, c** 1961–1990 and **b, d** 1996–2013. *Dark* (*light*) *shadings* indicate values significantly exceeding the 95% (90%) confidence level, estimated by Student's *t* test

Further results indicate that the interdecadal weakened connection between the SST_Indian and the northern Ferrell circulation is responsible for the weakened NECWP–SST_Indian relationship. During 1961–1990, the positive SST_Indian index is consistent with the significant northern Hadley and Ferrel cells. The SST_Indian might modulate the EU wave pattern and the NECWP by the northern meridional circulations. However, in 1996–2013, the connection between the SST_Indian and the northern Ferrel cell weakens. Therefore, the SST_Indian signal is faint over the Eurasian mid- to- high-latitudes. Hence, the relationship between the tropical Indian Ocean and the NECWP is disrupted. On the other hand, even though the SST_Atlantic-related SLP anomalies display the NAO pattern, the extent of the NAO enlarges eastward, and the anomalous magnitudes are remarkably enhanced after the mid-1990s. Such intensified air-sea interaction in the North Atlantic regions likely contributes to the strengthened NECWP–SST_Atlantic relationship. Furthermore, the interannual variability of the SST_Atlantic has strengthened around the mid-1990s, which might contribute to the strengthening of the interannual variability of the NECWP to some extent.

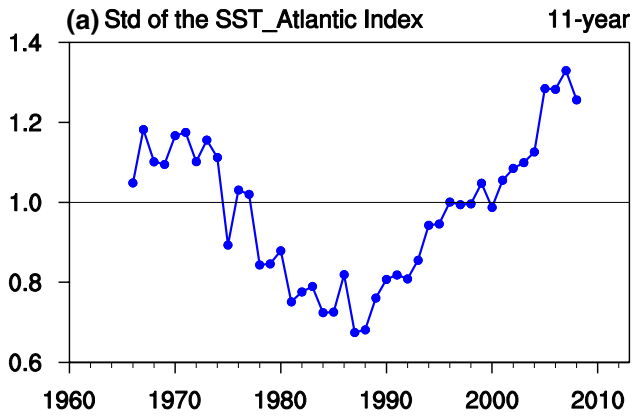


**Fig. 12** The 11-year-sliding standard deviation (Std) of the SST_Atlantic index for 1961–2013

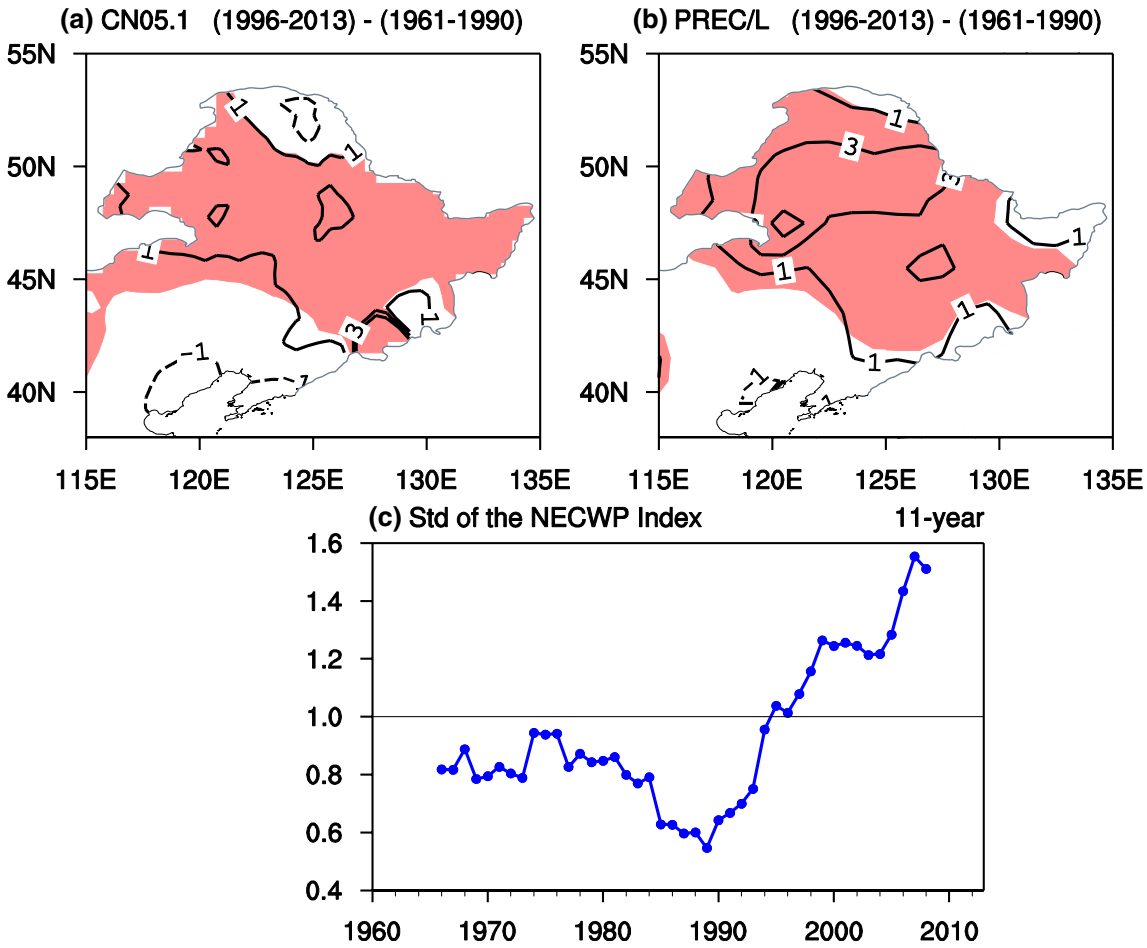


**Fig. 13** Differences (P2 minus P1) of the standard deviation for the winter precipitation between 1996 and 2013 (P2) and 1961–1990 (P1) based on **a** CN05.1 gridded data and **b** PREC/L data. Shades indicate values significantly exceeding the 95% confidence level as estimated by the *F* test. **c** The 11-year-sliding standard deviation of the NECWP index for 1961–2013

**Acknowledgements** This research was jointly supported by the National Natural Science Foundation of China (Grants 41421004 and 41210007) and the CAS–PKU Partnership Program.

## References

Bai RH (2001) Relation between sea surface temperature anomaly in the Atlantic and summer precipitation over the Northeast China. Marine Forecasts 18:50–57

Cao J, Lu RY, Hu JM, Wang H (2013) Spring Indian Ocean-western Pacific SST contrast and the East Asian summer rainfall anomaly. Adv Atmos Sci 30:1560–1568

Chang EC, Yeh SW, Hong SY, Wu RG (2013) Sensitivity of summer precipitation to tropical sea surface temperatures over East Asia in the GRIMs GMP. Geophys Res Lett 40:1824–1831

Chen MY, Xie PP, Janowiak JE, Arkin PA (2002) Global land precipitation: a 50 year monthly analysis based on gauge observations. J Hydrometeorology 3:249–266

Feldstein SB (2003) The dynamics of NAO teleconnection pattern growth and decay. Q J R Meteorol Soc 129:901–924

Feng X, Wang X, Wang Y (2006) Anomalies of the Northeast China floods season precipitation and SVD analysis with SSTA in world oceans. J Trop Meteor 22:367–373

Gao ZT, Hu ZZ, Zhu JS, Yang S, Zhang RH, Xiao ZN, Jha B (2014) Variability of summer rainfall in Northeast China and Its connection with spring rainfall variability in the Huang-Huai Region and Indian Ocean SST. J Clim 27:7086–7101

Geng QZ, Ding YH, Huang CY (1997) Influences of the extropical Pacific SST on the precipitation of the North China region. Adv Atmos Sci 14:339–349

Gong Q, Wang HY, Wang PX (2006) Analysis of climate and anomaly features of summer precipitation in Northeast China. Meteor Sci Tech 34:387–393

Guo QY (1983) East Asian summer monsoon strength index and its variation. Acta Geogr Sin 38:207–216

Han TT, Chen HP, Wang HJ (2015) Recent changes in summer precipitation in Northeast China and the background circulation. Int J Climatol 35:4210–4219

He JH, Wu ZW, Qi L, Jiang AJ (2006) Relationships among the Northern Hemisphere annual mode, the Northeast Cold Vortex and the summer rainfall in Northeast China. J Meteor Environ 22:1–5

Hu ZZ, Yang S, Wu RG (2003) Long-term climate variations in China and global warming signals. J Geophys Res 108:4614

Huang BY et al (2015) Extended reconstructed sea surface temperature version 4 (ERSST. V4). Part I: upgrades and intercomparisons. J Clim 28:911–930

Hurrell JW (1995) Decadal trends in the North Atlantic oscillation regional temperature and precipitation. Science 269:676–679

Kalnay E et al (1996) The NCEP/NCAR 40-year reanalysis project. Bull Am Meteorol Soc 77:437–471

Li SL, Hoerling MP, Peng SL (2006) Coupled ocean-atmosphere response to Indian Ocean warmth. Geophys Res Lett 33:L07713

Li Y, Wu BY, Yang QM, Huang SC (2013) Different relationships between spring SST in the Indian and Pacific oceans and summer precipitation in China. Acta Meteor Sin 27:509–520

Liu S, Wang N (2001) The impacts of antecedent ENSO event on air temperature over Northeast China in summer. J Trop Meteor 17:314–319

Liu ZX, Lian Y, Gao ZT, Shen BZ (2002) Analyses of the Northern Hemisphere circulation characters during northeast cold vortex persistence. Chin. J Atmos Sci 26:361–372

Peng SL, Rosinson WA, Li SH (2003) Mechanisms for the NAO responses to the North Atlantic SST tripole. J Clim 16:1987–2004

Plumb RA (1985) On the three-dimensional propagation of stationary waves. J Atmos Sci 42:217–229

Sardeshmukh PD, Hoskins BJ (1988) The generation of global rotational flow by steady idealized tropical divergence. J Atmos Sci 45:1228–1251

Shen BZ, Lian Y (2004) The preliminary analysis on the relationship between snow cover over the Tibetan Plateau and summer cold vortex precipitation in northeast China. J Jilin Univ Earth Sci 34:112–118

Shen BZ, Lin ZD, Lu RY, Lian Y (2011) Circulation anomalies associated with interannual variation of early- and late-summer precipitation in Northeast China. Sci China Earth Sci 54:1095–1104

Sun JQ, Wang HJ (2006) Regional difference of summer air temperature anomalies in Northeast China and its relationship to atmospheric general circulation and sea surface temperature. Chin J Geophys 49:662–671

Sun JQ, Wang HJ (2012) Changes of the connection between the summer North Atlantic oscillation and the East Asian summer rainfall. J Geophys Res 117:D08110

Sun B, Wang HJ (2015) Analysis of the major atmospheric moisture sources affecting three sub-regions of East China. Int J Climatol 35:2243–2257

Sun L, An G, Ding L, Shen BZ (2000) A climatic analysis of summer precipitation features and anomaly in Northeast China. Acta Meteor Sin 58:70–82

Sun L, An G, Lian Y, Gao ZT, Tang XL, Shen BZ, Ding L (2002) The unusual characteristics of general circulation in drought and waterlogging years of Northeast China. Clim. Environ Res 7:102–113

Sun JQ, Wang HJ, Yuan W (2008) Decadal variations of the relationship between the summer North Atlantic Oscillation and Middle East Asian air temperature. J Geophys Res 113:D15107

Tian BQ, Fan K (2013) Factors favorable to frequent extreme precipitation in the upper Yangtze River Valley. Meteorol Atmos Phys 121:189–197

Wang HJ, Chen HP (2012) Climate control for southeastern China moisture and precipitation: Indian or East Asian monsoon? J Geophys Res 117:D12109

Wang HJ, He SP (2013) The increase of snowfall in Northeast China after the mid-1980s. Chin Sci Bull 58:1350–1354

Wang HJ, He SP (2015) The North China/Northeastern Asia severe summer drought in 2014. J Clim 28:6667–6681

Watanabe M (2004) Asian jet waveguide and a downstream extension of the North Atlantic Oscillation. J Clim 17:4674–4691

Wu J, Gao XJ (2013) A gridded daily observation dataset over China region and comparison with the other datasets. Chin J Geophys 56:1102–1111

Wu RG, Hu ZZ, Kirtman BP (2003) Evolution of ENSO related rainfall anomalies in East Asia. J Clim 16:3742–3758

Wu RG, Yang S, Liu S, Sun L, Lian Y, Gao ZT (2010) Changes in the relationship between Northeast China summer temperature and ENSO. J Geophys Res 115:D21107

Wu RG, Yang S, Liu S, Sun L, Lian Y, Gao ZT (2011) Northeast China summer temperature and North Atlantic SST. J Geophys Res 116:D16116

Xu ZQ, Fan K (2012) Possible process for influences of winter and spring Indian Ocean SST anomalies interannual variability mode on summer rainfall over eastern China. Chin. J Atmos Sci 36:879–888

Xu ZQ, Fan K (2014) Simulating the mechanism of the interannual variability mode of the Indian Ocean sea surface temperature anomalies impacting on the summer rainfall over eastern China. Clim Environ Res 19:31–40

Xu ZQ, Fan K, Wang HJ (2015) Decadal variation of summer precipitation over China and associated atmospheric circulation after the late 1990s. J Clim 28:4086–4106

Yao XP, Dong M (2000) Research on the features of summer rainfall in Northeast China. Q J Applied Meteor 11:297–303

Zhou MZ, Wang HJ (2014) Late winter sea ice in the Bering Sea: prediction for Maize and Rice production in Northeast China. J Appl Meteor Climatol 53:1183–1192

Zhou MZ, Wang HJ, Yang S, Fan K (2013) Influence of springtime North Atlantic Oscillation on crops yields in Northeast China. Clim Dyn 41:3317–3324

Zhu YL (2011) A seasonal prediction model for the summer rainfall in Northeast China using the year-to-year increment approach. Atmos Oceanic Sci Lett 4:146–150